Electronic Supplementary Material (ESI) for Dalton Transactions.

Supplementary Information

Slow magnetic relaxation in Dy_2 and Dy_4 complexes of a versatile, trifunctional polydentate N,O-ligand

Muhammad U. Anwar,[a]* Ahmed Al-Harrasi,[a] Jeremy M. Rawson,[b]* Emma Gavey,[c] Jeffery Regier,[c] Dimitrios Alexandropoulos,[d] Melanie Pilkington[c] and Laurence K Thompson.[e]

[a]Natural and Medical Sciences Research Centre, University of Nizwa, P O Box 33, PC 616, Birkat Almouz. Nizwa, Oman, Email: usman.anwar@unizwa.edu.om

[b]Department of Chemistry and Biochemistry, University of Windsor, 401 Sunset Ave, Windsor ON, N9B3P4, Canada, Email: jmrawson@uniwndsor.ca

[c]Department of Chemistry, Brock University, 1812 Sir Isaac Brock Way. St Catharines, ON, L2S3A1, Canada, Email: mpilkington@brocku.ca

[d]Department of Materials, University of Oxford, 16 Parks Rd, OX1 3PH, Oxford, U.K.

[e]Department of Chemistry, Memorial University, St. John's, Newfoundland, A1B 3X7, Canada

Table of Contents

ESI-1: Crystallographic Studies

The structures of complexes **1** – **3** were solved by direct methods and non-H atoms refined anisotropically. The protonation state of each ligand was challenging to determine but was based on charge balance and hydrogen-bonding patterns. While there is likely to be some subtle changes in bond length on deprotonation (compare the two dominant resonance forms for the two anions shown below), the esd's on the experimentally observed bond lengths make such an analysis unreliable.

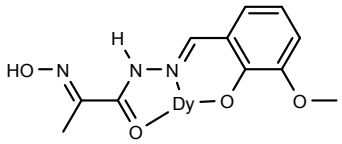

LH_2^-

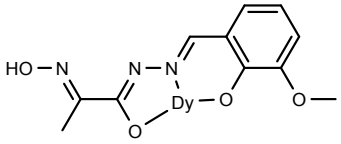

LH^{2-}

While Bond Valence Sum (BVS) calculations could potentially provide some insight into the protonation state of the ligand, they too derive from interatomic distances and BVS proved rather uninformative, consistent with the subtle changes in bond lengths in the ligand geometry which arise from the conjugated nature of the ligand system. Distinction between the different protonation states was therefore made primarily on the potential for hydrogen-bonding (Table S1):

- The N-H group in **L**H_2^- was invariably found to be a hydrogen bond donor
- The N lone pair in **L**H^{2-} was often not involved in hydrogen bonding at all or acted as a H-bond acceptor.

Table S1: Comparison of ligand geometries and H-bonding patterns for complexes **1** – **3**; **L**H^{2-} dianions are highlighted in grey and monoanions **L**H_2^- in white.

Complex	O-C	C-N	N-N	N-C	N-H…X	Assignment
1	1.244(4)	1.333(5)	1.394(5)	1.287(5)	N-H…O_{Et2O}	LH_2^-
	1.247(5)	1.326(5)	1.388(4)	1.288(5)	NH…ONO_2	LH_2^-
	1.240(5)	1.336(5)	1.393(4)	1.286(5)	NH…ONO_2	LH_2^-
	1.244(4)	1.329(5)	1.400(4)	1.290(5)	NH…O_{MeOH}	LH_2^-
2	1.26(1)	1.31(1)	1.43(1)	1.28(1)	N…HON	LH^{2-}
	1.23(1)	1.32(1)	1.39(1)	1.29(1)	None	LH^{2-}
	1.30(1)	1.31(1)	1.40(1)	1.31(1)	NH…OH_2[§]	LH_2^-
3	1.30(1)	1.30(1)	1.40(1)	1.30(1)	NH…OMe	LH_2^-
	1.33(1)	1.27(1)	1.41(1)	1.29(1)	None	LH^{2-}
	1.32(1)	1.28(1)	1.40(1)	1.29(1)	None	LH^{2-}

[§] The structure was treated with a solvent mask (SQUEEZE) due to disorder of the lattice water molecule over two positions. However both sites exhibit short N-H…O distance to **L**H_2^-. The deposited structure does not contain this lattice water but the extent of protonation was assigned based on the observed hydrogen bonding pattern prior to application of the solvent mask.

Table S2: Crystallographic Structural Data for complexes **1 – 3**

	1	**2**	**3**
Chemical formula	$C_{55}H_{80}Dy_2N_{14}O_{27}$	$C_{66}H_{70}Dy_4N_{18}O_{26}$	$C_{68}H_{74}Gd_4N_{18}O_{26}$
FW	1694.33	2181.40	2188.45
Crystal system,	Triclinic	Monoclinic	Triclinic
space group	P – 1	$P2_1/n$	P – 1
Temperature (K)	173(2)	173(2)	173(2)
a/Å	10.3755 (8)	14.7253 (10)	11.3795 (6)
b/ Å	14.3138 (11)	18.0284 (11)	12.1400 (6)
c/ Å	23.9924 (17)	14.9893 (10)	14.4181 (7)
α/°	92.068 (3)	90	85.283 (2)
β/°	95.604 (3)	91.787 (2)	75.253 (2)
γ/°	103.792 (3)	90	74.747 (2)
V/Å^3	3437.4 (4)	3977.3 (4)	1858.11 (16)
Z	2	2	1
D_c/Mgm^{-3}	1.637	1.821	1.956
Radiation type	Mo Kα	Cu *K*α	Mo Kα
μ(MoKα)/mm^{-1}	2.25	20.51	3.62
Independent reflns	9481	5342	6535
Reflns [I > 2σ(I)]	8535	4372	5024
R_{int}	0.035	0.053	0.063
θ_{max} (°)	22.954	58.945	25.000
R_1[a], wR_2[b]	0.024, 0.058	0.050, 0.133	0.043, 0.112
S[b]	1.11	1.02	1.11
Max/min residual e^- density (eÅ^{-3})	+1.15 −0.70	+1.98 −0.81	+3.47 -1.47
CCDC	1919889	1919888	1919890

[a] $I > 2\sigma(I)$, [b] all data

Table S3: Selected bond lengths (Å) and bond angles (°) for complex **1**

Bond	Distances	Bond	Distance
Dy1—O2	2.183 (2)	Dy2—O6	2.185 (3)
Dy1—O10	2.273 (2)	Dy2—O14	2.307 (2)
Dy1—O14	2.341 (2)	Dy2—O10	2.357 (2)
Dy1—O3	2.350 (2)	Dy2—O7	2.387 (3)
Dy1—O11	2.401 (3)	Dy2—O15	2.416 (3)
Dy1—N1	2.522 (3)	Dy2—N4	2.557 (3)
Dy1—N7	2.573 (3)	Dy2—N10	2.577 (3)
Dy1—O28	2.630 (3)	Dy2—O28	2.600 (2)
Dy1—O13	2.672 (2)	Dy2—O9	2.621 (3)

Bond	Angles	Bond	Angles
O2—Dy1—O10	85.58 (9)	O6—Dy2—O14	84.73 (9)
O2—Dy1—O14	117.89 (9)	O6—Dy2—O10	122.28 (9)
O10—Dy1—O14	70.62 (8)	O14—Dy2—O10	69.76 (8)
O2—Dy1—O3	130.26 (9)	O6—Dy2—O7	130.02 (9)
O10—Dy1—O3	139.31 (9)	O14—Dy2—O7	139.18 (9)
O14—Dy1—O3	74.73 (9)	O10—Dy2—O7	72.76 (9)
O2—Dy1—O11	114.96 (9)	O6—Dy2—O15	110.00 (9)
O10—Dy1—O11	117.26 (9)	O14—Dy2—O15	121.92 (9)
O14—Dy1—O11	127.05 (9)	O10—Dy2—O15	127.57 (9)
O3—Dy1—O11	69.30 (9)	O7—Dy2—O15	71.12 (9)
O2—Dy1—N1	70.82 (10)	O6—Dy2—N4	69.78 (10)
O10—Dy1—N1	155.62 (9)	O14—Dy2—N4	154.51 (9)
O14—Dy1—N1	125.61 (9)	O10—Dy2—N4	123.73 (9)
O3—Dy1—N1	64.76 (10)	O7—Dy2—N4	64.16 (9)
O11—Dy1—N1	69.89 (10)	O15—Dy2—N4	69.58 (10)
O2—Dy1—N7	75.85 (10)	O6—Dy2—N10	74.78 (10)
O10—Dy1—N7	68.44 (9)	O14—Dy2—N10	68.79 (9)
O14—Dy1—N7	135.37 (9)	O10—Dy2—N10	132.86 (9)
O3—Dy1—N7	131.15 (9)	O7—Dy2—N10	133.30 (9)

O11—Dy1—N7	61.90 (9)	O15—Dy2—N10	62.61 (9)
N1—Dy1—N7	98.95 (10)	N4—Dy2—N10	103.25 (10)
O2—Dy1—O28	147.27 (9)	O6—Dy2—O28	147.12 (9)
O10—Dy1—O28	64.32 (8)	O14—Dy2—O28	66.64 (8)
O14—Dy1—O28	65.68 (8)	O10—Dy2—O28	63.79 (8)
O3—Dy1—O28	82.47 (8)	O7—Dy2—O28	82.78 (8)
O11—Dy1—O28	72.12 (8)	O15—Dy2—O28	75.04 (8)
N1—Dy1—O28	136.42 (9)	N4—Dy2—O28	137.48 (9)
N7—Dy1—O28	81.02 (9)	N10—Dy2—O28	79.79 (9)
O2—Dy1—O13	74.04 (9)	O6—Dy2—O9	76.47 (9)
O10—Dy1—O13	106.88 (8)	O14—Dy2—O9	102.98 (8)
O14—Dy1—O13	60.90 (8)	O10—Dy2—O9	61.37 (8)
O3—Dy1—O13	72.71 (8)	O7—Dy2—O9	71.73 (9)
O11—Dy1—O13	135.23 (8)	O15—Dy2—O9	134.84 (9)
N1—Dy1—O13	73.09 (9)	N4—Dy2—O9	71.66 (9)
N7—Dy1—O13	149.81 (9)	N10—Dy2—O9	150.67 (9)
O28—Dy1—O13	125.13 (8)	O28—Dy2—O9	124.07 (8)

Table S4: Continuous Shape Measures calculation of Dy1 and Dy2 in complex **1** (geometries which give the smallest deviation from the experimental structure are highlighted).

	JCSAPR-9 Capped square antiprism J10 **(C_{4v})**	CSAPR-9 Spherical capped square antiprism **(C_{4v})**	JTCTPR-9 Tricapped trigonal prism J51 **(D_{3h})**	TCTPR-9 Spherical tricapped trigonal prism **(D_{3h})**	MFF-9 Muffin **(C_s)**
Dy1	3.36	1.97	5.13	1.73	1.760
Dy2	2.85	1.73	4.43	1.54	1.95

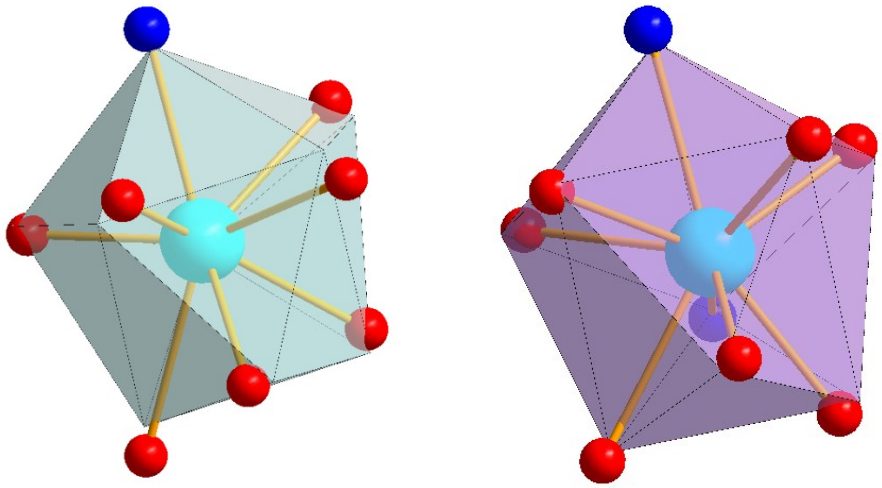

(a) (b)

Figure S1: Calculated polyhedron for Dy1 (a: Spherical tricapped trigonal prism) and for Dy2 (b: Spherical tricapped trigonal prism (D_{3h}) in complex **1**.

Table S5: Selected bond lengths (Å) and bond angles (°) for complex **2**

Bond	Distances	Bond	Distances
Dy1—O2	2.241 (5)	Dy2—O6	2.259 (6)
Dy1—O10	2.311 (6)	Dy2—O7	2.323 (5)
Dy1—O7	2.334 (6)	Dy2—O13	2.362 (6)
Dy1—O13i	2.338 (5)	Dy2—O11i	2.405 (6)
Dy1—O3	2.361 (5)	Dy2—O10i	2.431 (5)
Dy1—O13	2.512 (5)	Dy2—O3	2.488 (5)
Dy1—N1	2.529 (7)	Dy2—N4	2.549 (8)
Dy1—N6	2.653 (7)	Dy2—N7i	2.556 (7)
		Dy2—N3	2.679 (8)

Bond	Angles	Bond	Angles
O2—Dy1—O10	86.2 (2)	C8—N1—N2	112.8 (7)
O2—Dy1—O7	119.2 (2)	C8—N1—Dy1	130.1 (6)
O10—Dy1—O7	148.95 (19)	O6—Dy2—O7	123.5 (2)
O2—Dy1—O13i	110.66 (19)	O6—Dy2—O13	158.5 (2)
O10—Dy1—O13i	70.52 (19)	O7—Dy2—O13	75.33 (19)
O7—Dy1—O13i	83.07 (19)	O6—Dy2—O11i	84.3 (2)
O2—Dy1—O3	116.77 (19)	O7—Dy2—O11i	150.9 (2)
O10—Dy1—O3	124.72 (19)	O13—Dy2—O11i	75.81 (19)
O7—Dy1—O3	62.24 (19)	O6—Dy2—O10i	125.1 (2)
O13i—Dy1—O3	130.45 (18)	O7—Dy2—O10i	70.57 (18)
O2—Dy1—O13	168.5 (2)	O13—Dy2—O10i	68.09 (18)
O10—Dy1—O13	83.09 (18)	O11i—Dy2—O10i	101.91 (19)
O7—Dy1—O13	72.33 (18)	O6—Dy2—O3	110.9 (2)
O13i—Dy1—O13	69.57 (19)	O7—Dy2—O3	60.47 (18)
O3—Dy1—O13	66.88 (17)	O13—Dy2—O3	67.26 (18)
O2—Dy1—N1	70.4 (2)	O11i—Dy2—O3	104.18 (19)
O10—Dy1—N1	84.3 (2)	O10i—Dy2—O3	119.67 (18)
O7—Dy1—N1	119.5 (2)	O6—Dy2—N4	69.9 (2)
O13i—Dy1—N1	154.5 (2)	O7—Dy2—N4	62.2 (2)
O3—Dy1—N1	61.7 (2)	O13—Dy2—N4	131.6 (2)
O13—Dy1—N1	104.2 (2)	O11i—Dy2—N4	145.2 (2)
O2—Dy1—N6	65.8 (2)	O10i—Dy2—N4	76.4 (2)
O10—Dy1—N6	126.9 (2)	O3—Dy2—N4	106.6 (2)
O7—Dy1—N6	59.6 (2)	O6—Dy2—N7i	71.8 (2)
O13i—Dy1—N6	78.37 (19)	O7—Dy2—N7i	130.5 (2)
O3—Dy1—N6	108.3 (2)	O13—Dy2—N7i	104.9 (2)
O13—Dy1—N6	124.5 (2)	O11i—Dy2—N7i	61.9 (2)
N1—Dy1—N6	122.1 (2)	O10i—Dy2—N7i	64.6 (2)
C2—O1—C1	118.6 (8)	O3—Dy2—N7i	165.9 (2)
C7—O2—Dy1	139.6 (6)	N4—Dy2—N7i	87.4 (2)
C9—O3—Dy1	118.7 (6)	O6—Dy2—N3	65.4 (2)
C9—O3—Dy2	124.3 (5)	O7—Dy2—N3	113.8 (2)
Dy1—O3—Dy2	98.00 (18)	O13—Dy2—N3	98.8 (2)
N3—O4—H4	31 (2)	O11i—Dy2—N3	67.1 (2)
C13—O5—C12	116.6 (11)	O10i—Dy2—N3	165.2 (2)
C18—O6—Dy2	133.9 (6)	O3—Dy2—N3	57.2 (2)
Dy2—O13—Dy1	97.29 (18)	N4—Dy2—N3	118.3 (2)
Dy1i—O13—H13	112.9	N7i—Dy2—N3	114.9 (2)
Dy2—O13—H13	112.9	C20—O7—Dy2	124.9 (5)
N2—N1—Dy1	116.7 (5)	C20—O7—Dy1	131.1 (5)
C31—O11—Dy2i	120.3 (6)	Dy2—O7—Dy1	103.6 (2)
N9—O12—H12	106 (8)	N6—O—H	109 (7)
Dy1i—O13—Dy2	109.3 (2)	C24—O9—C23	115.6 (7)
Dy1i—O13—Dy1	110.43 (19)	C29—O10—Dy1	128.1 (5)
Dy1—O13—H13	112.9	C29—O10—Dy2i	122.2 (5)
		Dy1—O10—Dy2i	107.9 (2)

Table S6: Continuous Shape Measures calculation of Dy1(Dy1*) and Dy2(Dy2*) in complex **2** (geometries which give the smallest deviation from the experimental structure are highlighted).

	Triangular dodecahedron **(D_{2d})**	Johnson gyrobifastigium J26 **(D_{2d})**	Biaugmented trigonal prism J50 **(C_{2v})**	Biaugmented trigonal prism **(C_{2v})**	Snub diphenoid J84 **(D_{2d})**
Dy1(Dy1*)	8.87942	7.37	8.59	7.25	9.35
	Capped cube J8 (C_{4v})	**Spherical-relaxed capped cube (C_{4v})**	**Spherical capped square antiprism (C_{4v})**	**Hula-hoop (C_{2v})**	**Muffin (C_s)**
Dy2(Dy2*)	5.26	3.74	9.57682	5.79932	8.69263

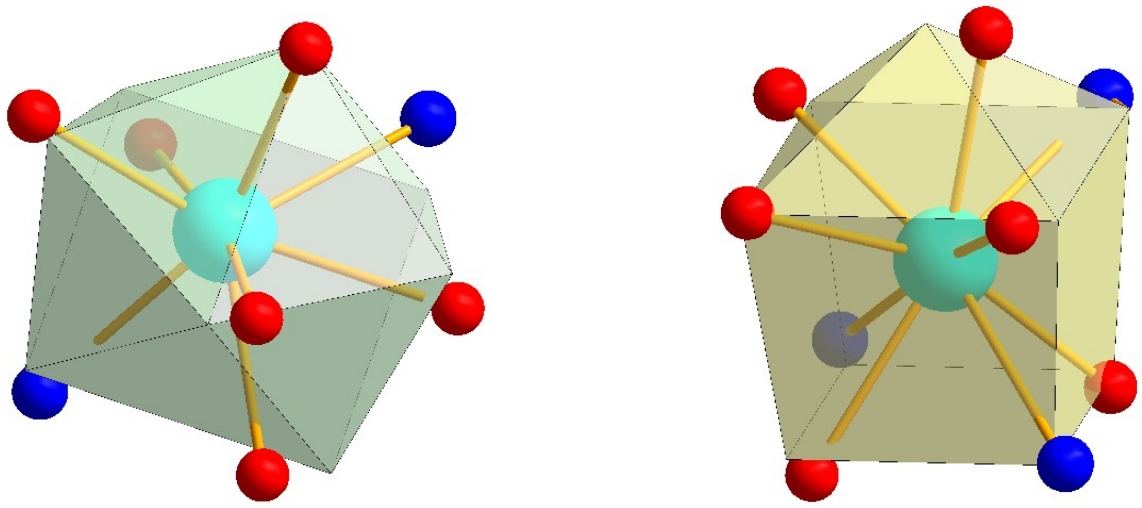

Figure S2: Calculated polyhedron for Dy1Dy1* (left) and Dy2Dy2* (Right) in complex **2**.

Table S7: Selected bond lengths (Å) and bond angles (°) for complex **3**

Bond	Distances	Bond	Distances
Gd1—O52	2.234 (6)	Gd2—O12	2.249 (6)
Gd1—O53	2.315 (6)	Gd2—O32	2.376 (6)
Gd1—O32	2.392 (6)	Gd2—O13	2.388 (6)
Gd1—O13i	2.426 (6)	Gd2—O53i	2.451 (6)
Gd1—N51	2.465 (8)	Gd2—O33i	2.459 (5)
Gd1—O33i	2.489 (6)	Gd2—N31	2.578 (7)
Gd1—O71	2.547 (6)	Gd2—N11	2.600 (7)
Gd1—N33i	2.575 (8)	Gd2—O33	2.780 (6)
Gd1—N13i	2.590 (8)	Gd2—N53i	2.781 (8)
N13—Gd1i	2.590 (8)	O13—Gd1i	2.426 (6)

Bond	Angles	Bond	Angles
O52—Gd1—O53	140.6 (2)	O53i—Gd2—N31	122.8 (2)
O52—Gd1—O32	90.6 (2)	O33i—Gd2—N31	98.6 (2)
O53—Gd1—O32	86.9 (2)	O12—Gd2—N11	68.3 (2)
O52—Gd1—O13i	136.4 (2)	O32—Gd2—N11	100.9 (2)
O53—Gd1—O13i	65.9 (2)	O13—Gd2—N11	60.3 (2)
O32—Gd1—O13i	130.83 (19)	O53i—Gd2—N11	118.0 (2)
O52—Gd1—N51	75.4 (2)	O33i—Gd2—N11	167.0 (2)
O53—Gd1—N51	65.7 (2)	N31—Gd2—N11	69.1 (2)
O32—Gd1—N51	77.7 (2)	O33—Gd2—N53i	121.4 (2)
O13i—Gd1—N51	120.5 (2)	O12—Gd2—O32	79.1 (2)
O52—Gd1—O33i	140.8 (2)	O12—Gd2—O13	115.9 (2)
O53—Gd1—O33i	73.42 (19)	O32—Gd2—O13	143.48 (19)
O32—Gd1—O33i	68.48 (19)	O12—Gd2—O53i	117.1 (2)
O13i—Gd1—O33i	64.88 (19)	O32—Gd2—O53i	140.95 (19)
N51—Gd1—O33i	127.6 (2)	O13—Gd2—O53i	64.43 (19)
O52—Gd1—O71	80.2 (2)	O12—Gd2—O33i	116.2 (2)
O53—Gd1—O71	80.9 (2)	O32—Gd2—O33i	69.22 (19)
O32—Gd1—O71	147.17 (19)	O13—Gd2—O33i	122.58 (19)
O13i—Gd1—O71	70.59 (19)	O53i—Gd2—O33i	71.81 (19)
N51—Gd1—O71	69.5 (2)	O12—Gd2—N31	117.4 (2)
O33i—Gd1—O71	134.55 (19)	O32—Gd2—N31	66.5 (2)
O52—Gd1—N33i	80.9 (2)	O13—Gd2—N31	77.3 (2)
O53—Gd1—N33i	134.3 (2)	O53i—Gd2—O33	66.33 (18)
O32—Gd1—N33i	71.4 (2)	O33i—Gd2—O33	68.73 (19)
O13i—Gd1—N33i	98.5 (2)	N31—Gd2—O33	58.1 (2)
N51—Gd1—N33i	140.5 (3)	N11—Gd2—O33	106.2 (2)
O33i—Gd1—N33i	61.4 (2)	O12—Gd2—N53i	63.1 (2)
O71—Gd1—N33i	136.5 (2)	O32—Gd2—N53i	112.6 (2)
O52—Gd1—N13i	80.1 (2)	O13—Gd2—N53i	103.7 (2)
O53—Gd1—N13i	124.5 (2)	O53i—Gd2—N53i	57.1 (2)
O32—Gd1—N13i	139.2 (2)	O33i—Gd2—N53i	80.1 (2)
O13i—Gd1—N13i	60.2 (2)	N31—Gd2—N53i	178.6 (2)
N51—Gd1—N13i	135.7 (2)	N11—Gd2—N53i	112.2 (2)
O33i—Gd1—N13i	94.2 (2)	O12—Gd2—O33	174.4 (2)
O71—Gd1—N13i	70.4 (2)	O32—Gd2—O33	101.00 (18)
N33i—Gd1—N13i	67.9 (2)	O13—Gd2—O33	60.79 (18)
C19—O13—Gd1i	127.5 (5)	C18—N11—N12	113.1 (7)
C20—N13—Gd1i	125.1 (6)	C18—N11—Gd2	129.3 (6)
O14—N13—Gd1i	120.0 (5)	N12—N11—Gd2	117.0 (5)
Gd2—O13—Gd1i	105.4 (2)	C17—O12—Gd2	141.8 (6)
C20—N13—O14	114.6 (7)	C19—O13—Gd2	121.8 (5)
C19—N12—N11	110.2 (7)	O11—C12—C13	126.6 (10)
C19—N12—H12	124.9	O11—C12—C17	112.2 (9)
N11—N12—H12	124.9	C13—C12—C17	121.2 (11)

Table S8: Continuous Shape Measures calculation of Gd1(Gd1*) and Gd2(Gd2*) in complex **3** (geometries which give the smallest deviation from the experimental structure are highlighted).

	Capped square antiprism J10 (C_{4v})	**Spherical capped square antiprism (C_{4v})**	**Tricapped trigonal prism J51 (D_{3h})**	**Spherical tricapped trigonal prism (D_{3h})**	**Muffin (C_s)**
Gd1(Gd1*)	1.69	0.67	3.04	1.62	0.56
	Capped cube J8 (C_{4v})	**Spherical-relaxed capped cube (C_{4v})**	**Spherical capped square antiprism (C_{4v})**	**Hula-hoop (C_{2v})**	**Muffin (C_s)**
Gd2(Gd2*)	4.57	2.90	10.65	7.03	9.30

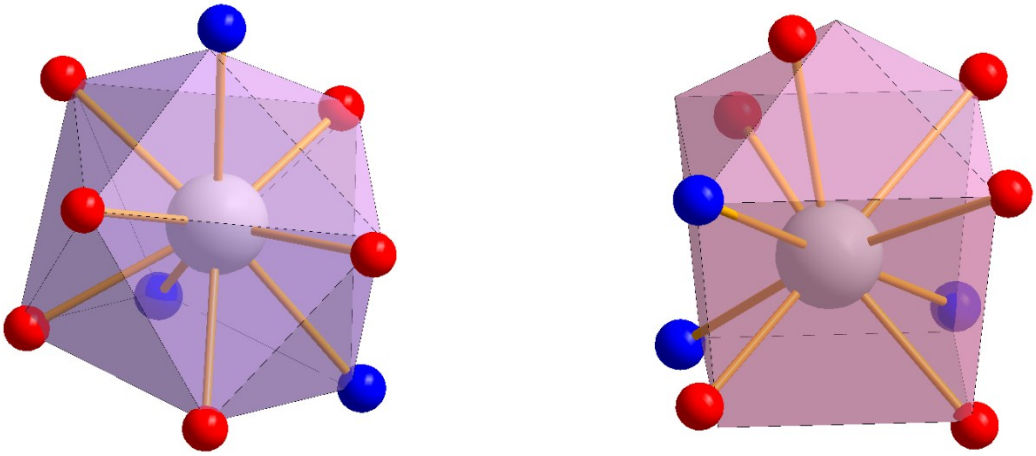

Figure S3: Calculated polyhedron for Gd1Gd1* (left) and Gd2Gd2* (Right) in complex **3**

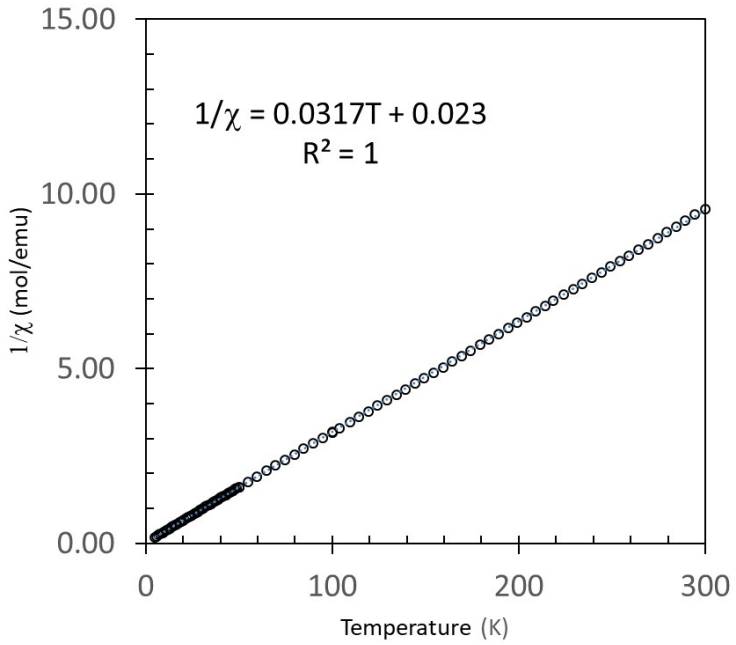

Figure S4: Temperature dependence of 1/χ for **3** with dotted line representing the fit to Curie-Weiss

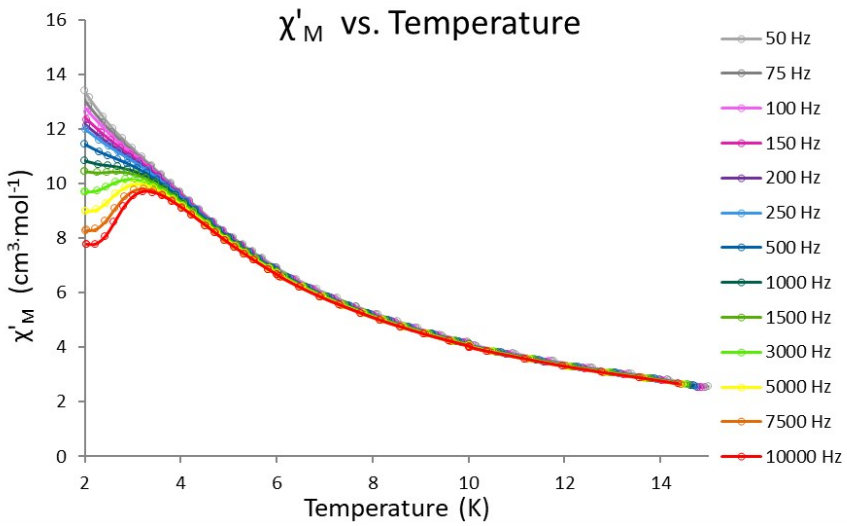

Figure S5. Temperature dependence of in-phase χ' (ac susceptibility signals for 1 in an optimal applied dc field of 1000 Oe.

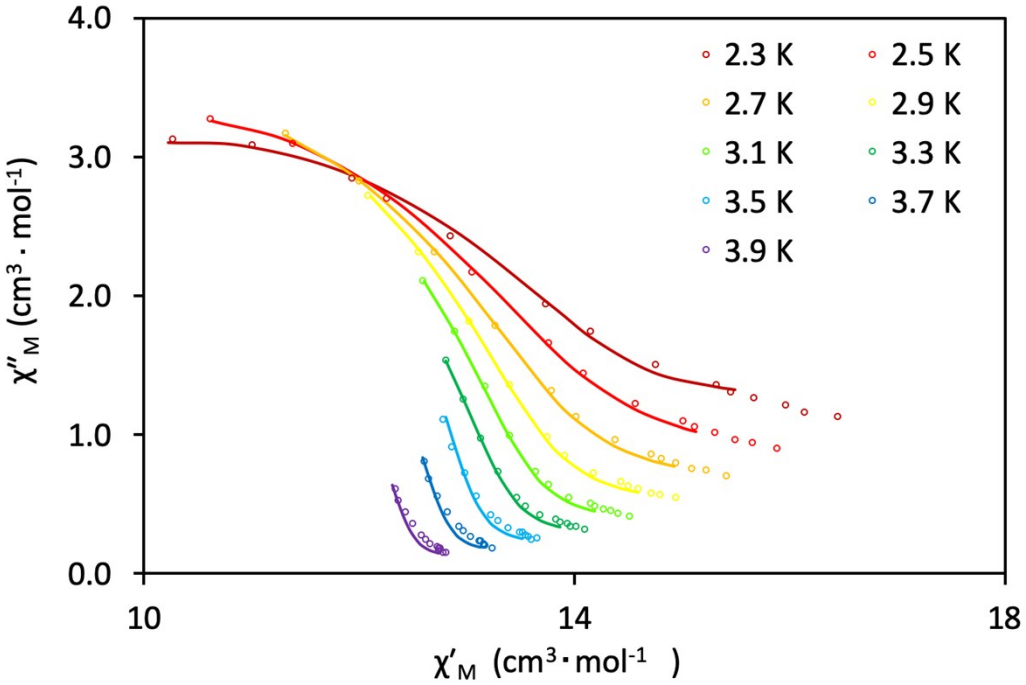

Figure S6: Cole-Cole plot for **1**, solid line represents the best fitted parameter.

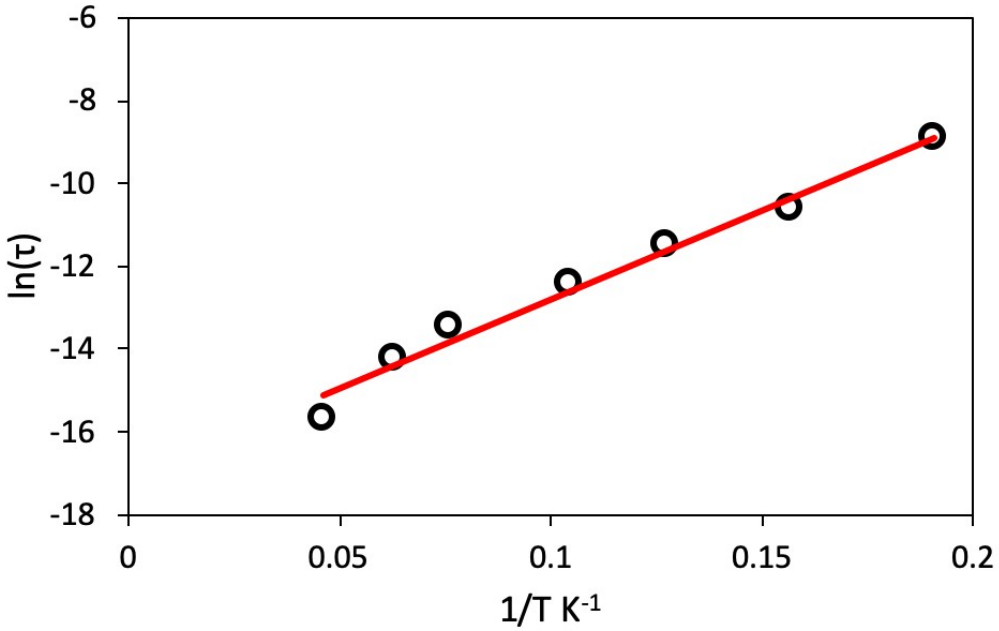

Figure S7: ln(τ) *vs* 1/T plot for complex **1**. Red line represents the fit to the Arrhenius equation.

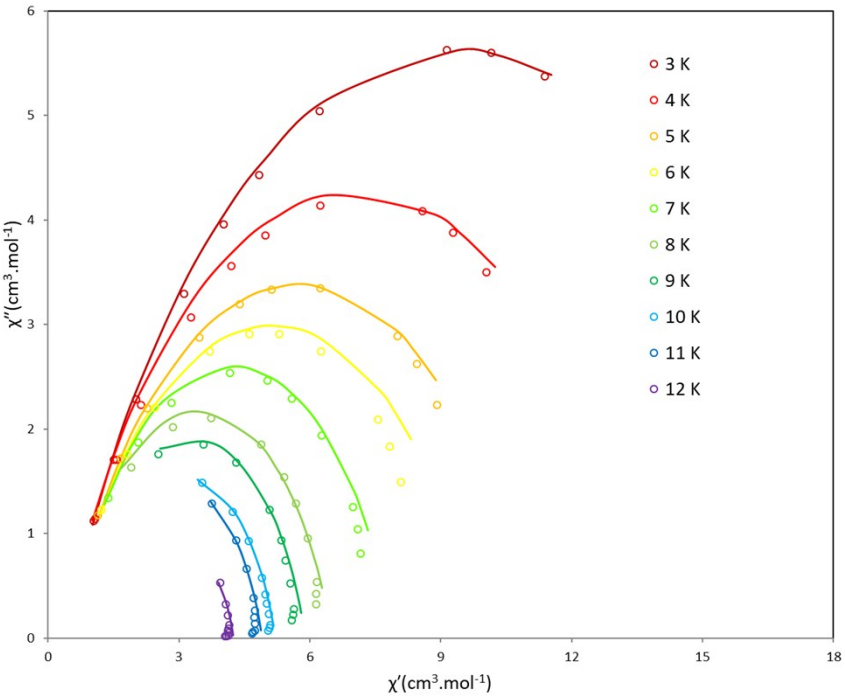

Figure S8: Cole-Cole plot for **2**, solid line represents the best fitted parameter.

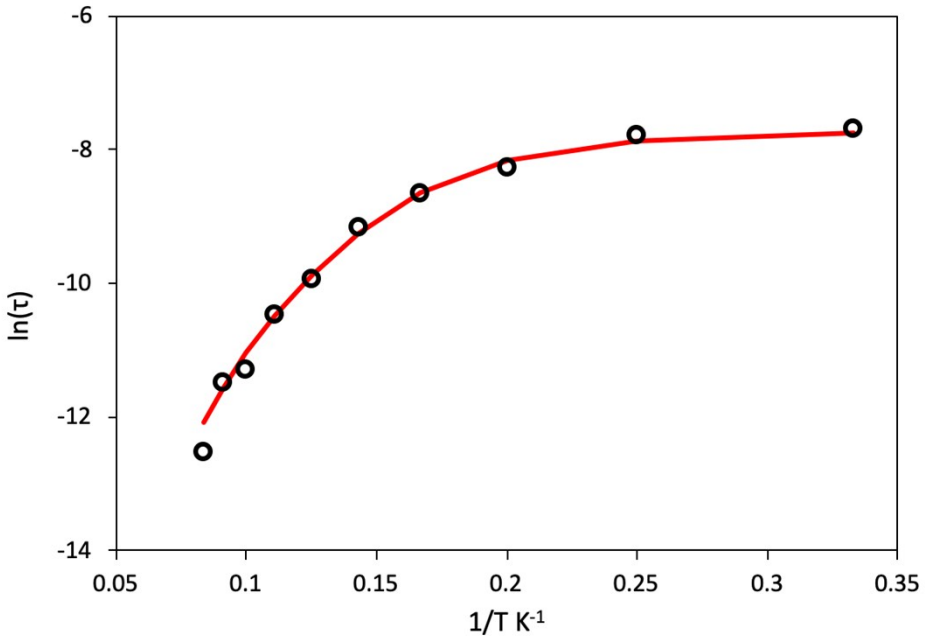

Figure S9: ln(τ) *vs* 1/T plot for complex **2**. Red line represents the fit to equation 2.